EXPLOITING HIDDEN PILOTS FOR CARRIER FREQUENCY OFFSET ESTIMATION FOR GENERALIZED MC-CDMA SYSTEMS

Yi Ma and Rahim Tafazolli

Center for communication systems research,
The University of Surrey, U.K. GU2 9SE
Email: y.ma,r.tafazolli@surrey.ac.uk

ABSTRACT

This paper proposes a novel carrier frequency offset (CFO) estimation method for generalized MC-CDMA systems in unknown frequency-selective channels utilizing hidden pilots. It is established that CFO is identifiable in the frequency-domain by employing cyclic statistics (CS) and linear regression (LR) algorithms. We show that the CS-based estimator is capable of mitigating the normalized CFO (NCFO) to a small error value. Then, the LR-based estimator can be employed to offer more accurate estimation by removing the residual quantization error after the CS-based estimator.

1. INTRODUCTION

Generalized multicarrier code-division multiple access (GMC-CDMA) has recently received increasing interests for high data rate transmissions [1]-[2]. Relying on the precoding redundancy, [1] has shown that signal recovery for GMC-CDMA systems is independent of channel null (deep fade) locations. Hence, for uncoded systems, GMC-CDMA outperforms the conventional MC-CDMA in frequency-selective fading channels. As an orthogonal frequency-division multiplexing (OFDM) based technique, GMC-CDMA is very sensitive to carrier frequency offset (CFO) [3]. A good CFO estimator is acquired to improve the overall system performance. In literatures, many data-aided and non data-aided CFO estimators have been reported for multicarrier systems (e.g. [6]-[10]). However, very few publications have addressed so far on exploiting hidden pilots for the CFO estimation. This motivated us to develop a novel CFO estimator by using hidden pilots.

Originally, techniques using hidden pilots were proposed for low-complexity estimation of static channels (or slowly time-varying channels) in single-carrier systems (see [4], [5]). In this paper, we deploy the hidden pilots in the GMC-CDMA system for the accurate CFO estimation. The proposed CFO estimator consists of two sub-estimators operating in the frequency domain. Using the cyclic-statistics (CS) algorithm, the first sub-estimator is able to mitigate the normalized CFO (NCFO) to a small error value. This error is mainly from the quantization noise in the CS-based sub-estimator. The second sub-estimator is based on the linear-regression (LR) algorithm. It is shown that the LR-based estimator performs well for the case of small NCFO, and is a good compensation to the CS-based estimator. Simulation results are provided to confirm our theoretical analysis.

The work in this paper was supported by EU-IST 4More, No. IST-2002-507039.

2. GMC-CDMA WITH HIDDEN PILOTS

The discrete-time equivalent model for the downlink of GMC-CDMA system has been presented in [1], [2]. Considering the CFO, Fig. 1 depicts the downlink GMC-CDMA model with hidden pilots. Prior to transmission, the information-bearing symbols are grouped into blocks $\mathbf{s}_M(n)$ with the size of $M \times 1$, where n denotes the block index. Then, these blocks are fed to a $K \times M$ block precoder $\mathbf{\Theta}$ to produce blocks $\mathbf{s}_K(n) = \mathbf{\Theta}\mathbf{s}_M(n)$. In the GMC-CDMA system, $\mathbf{\Theta}$ is used for the user signatures and also introduce the precoding redundancy ($K > M$) [1]. Let $L_t = K - M$, we construct another block precoder $\mathbf{\Theta}_t$ with the size of $K \times L_t$. This precoder is used to precode the hidden-pilot blocks $\mathbf{p}(n)$, with the input-output relationship of $\tilde{\mathbf{p}}(n) = \mathbf{\Theta}_t\mathbf{p}(n)$. Then, we feed the sum of $\mathbf{s}_K(n)$ and $\tilde{\mathbf{p}}(n)$ to the CP-OFDM modulator $\mathbf{F}$. The matrix $\mathbf{F} = [\mathbf{F}_{\rm cp}^T,\ \mathbf{F}_K^T]^T$ has the size of $J \times K$ ($J = K + L_{\rm cp}$), where $L_{\rm cp}$ denotes the length of cyclic prefix (CP); $(\cdot)^T$ denotes the matrix transpose; $\mathbf{F}_K$ denotes the inverse discrete Fourier transform (IDFT) matrix with the size of $K \times K$; $\mathbf{F}_{\rm cp}$ is formed by collecting the last $L_{\rm cp}$ rows of $\mathbf{F}_K$. The output of CP-OFDM modulator (or transmitted block) is given by

$$\mathbf{x}(n) = \mathbf{F}\mathbf{W}[\mathbf{s}_M^T(n), \mathbf{p}^T(n)]^T \qquad (1)$$

where $\mathbf{W} = [\mathbf{\Theta}, \mathbf{\Theta}_t]$ is usually formed by a Walsh matrix in GMC-CDMA systems. The detail description on how to obtain the output (1) can be found in [1].

The transmitted blocks experience the propagation channel $\mathbf{h} = [h(0), h(1), \cdots, h(L_u)]^T$, where L_u denotes the

upper bound of the channel order. Considering the CFO, the received blocks can be formulated as (see [1], [6])

$$\mathbf{y}_J(n) = \mathbf{\Omega}_J\mathbf{H}_l\mathbf{x}(n) + \underbrace{\mathbf{\Omega}_J\mathbf{H}_u\mathbf{x}(n-1)}_{\text{IBI}} + \mathbf{v}_J(n) \quad (2)$$

where $\mathbf{H}_l$ and $\mathbf{H}_u$ are $J \times J$ lower and upper triangular matrices with entries $[\mathbf{H}_l]_{n,k} = h(n-k)$ and $[\mathbf{H}_u]_{n,k} = h(J+n-k)$. $\mathbf{v}_J(n)$ is the zero-mean Gaussian noise with the size of $J\times 1$; The diagonal matrix $\mathbf{\Omega}_J = \text{diag}\{\Phi^{nJ}, \Phi^{nJ+1}, \cdots, \Phi^{(n+1)J-1}\}$ comprises the CFO information with $\Phi = \exp(j\frac{2\pi}{K}\phi)$, where ϕ denotes the CFO normalized by the subcarrier spacing Δf. Normally, for the CP length $L_{\text{cp}} \geqslant L_u$, the inter-block interference (IBI) part can be removed by discarding CP at the receiver, and the remaining part becomes

$$\mathbf{y}_K(n) = \mathbf{\Omega}_K\mathbf{C}_K\mathbf{F}_K\mathbf{W}[\mathbf{s}_M^T(n), \mathbf{p}^T(n)]^T + \mathbf{v}_K(n) \quad (3)$$

where $\mathbf{\Omega}_K = \text{diag}\{\Phi^{nJ+L_{\text{cp}}}, \Phi^{nJ+L_{\text{cp}}+1}, \cdots, \Phi^{(n+1)J-1}\}$, $\mathbf{C}_K$ is the circulant channel matrix addressed in [1], $\mathbf{v}_K(n)$ is the corresponding noise vector. We perform the DFT on $\mathbf{y}_K(n)$ and obtain the frequency-domain blocks as

$$\begin{aligned}\tilde{\mathbf{y}}_K(n) &= \Phi^{nJ+L_{\text{cp}}}(\boldsymbol{\mathcal{D}}_K\mathbf{W}[\mathbf{s}_M^T(n), \mathbf{p}^T(n)]^T + \mathbf{i}_{\mathbf{s}}(n) \\ &+ \mathbf{i}_{\mathbf{p}}(n)) + \tilde{\mathbf{v}}_K(n) \quad (4)\end{aligned}$$

where $\bar{\mathbf{\Omega}}_K = \text{diag}\{\Phi^0, \Phi^1, \cdots, \Phi^{K-1}\}$, $\tilde{\mathbf{v}}_K(n) = \mathbf{F}_K^{-1}\mathbf{v}_K(n)$; $\mathbf{i}_{\mathbf{s}}(n)$ and $\mathbf{i}_{\mathbf{p}}(n)$ are the inter-carrier interferences (ICIs) contributed by the information symbols and pilots respectively; $\boldsymbol{\mathcal{D}}_K = \mathbf{D}(\tilde{\mathbf{h}})$, where $\tilde{\mathbf{h}}$ denotes the channel frequency-response (CFR) with the size of $K \times 1$, and $\mathbf{D}(\mathbf{a})$ denotes the diagonal matrix with $\mathbf{a}$ in its diagonal. Then, we have three comments on (4):

1) The pilot blocks are assumed to be invariant with respect to the block index n. So, we can omit the index n in pilot-related terms $\tilde{\mathbf{p}}(n)$, $\mathbf{p}(n)$ and $\mathbf{i}_{\mathbf{p}}(n)$ for convenience;

2) The ICI term $\mathbf{i}_{\mathbf{s}}(n)$ is contributed by $\mathbf{s}(n)$, and thus has the zero-mean and is uncorrelated for the block index n [3];

3) When ϕ and $\mathbf{h}$ are known at the receiver, the CFO and pilot blocks can be eliminated from (3). Then, the zero-forcing (ZF) equalization can be employed in the frequency-domain. [1] has shown that $\boldsymbol{\mathcal{D}}_K$ has at most L_u zeros on its diagonal, so the signal recovery is independent of channel null (deep fade) locations only when $L_t \geqslant L_u$ and any M rows of $\mathbf{\Theta}$ are linear independent;

Later on, we present how to use hidden pilots for the CFO estimation.

3. ESTIMATION OF CFO

3.1. The CS-based estimator

Using the CS algorithm for the CFO estimation was originally proposed in [12], where the pulse-shaping filter at the transmitter plays the key role to introduce the cyclic spectrum. Then, this method was applied in multicarrier systems [9]. In our method, the cyclic-spectrum is enabled by the hidden pilots.

We start the analysis from the autocorrelation of the received blocks (4), and obtain the correlation matrix as

$$\begin{aligned}&\boldsymbol{\mathcal{C}}_{\tilde{\mathbf{y}}_K\tilde{\mathbf{y}}_K}(n, n_\tau) \\ =\ &\mathcal{E}\{\tilde{\mathbf{y}}_K(n+n_\tau)\tilde{\mathbf{y}}_K^{\mathcal{H}}(n)\} \\ =\ &\Phi^{n_\tau J}(\boldsymbol{\mathcal{D}}_K(\mathbf{\Theta}\boldsymbol{\mathcal{C}}_{\mathbf{s}_M\mathbf{s}_M}(n_\tau)\mathbf{\Theta}^{\mathcal{H}} + \boldsymbol{\mathcal{C}}_{\tilde{\mathbf{p}}\tilde{\mathbf{p}}})\boldsymbol{\mathcal{D}}_K^{\mathcal{H}} \\ &+\boldsymbol{\mathcal{D}}_K(\mathbf{\Theta}\boldsymbol{\mathcal{C}}_{\mathbf{s}_M\mathbf{i}_s}(n_\tau) + \boldsymbol{\mathcal{C}}_{\tilde{\mathbf{p}}\mathbf{i}_{\mathbf{p}}}) + (\boldsymbol{\mathcal{C}}_{\mathbf{s}_M\mathbf{i}_s}^{\mathcal{H}}(n_\tau)\mathbf{\Theta}^{\mathcal{H}} \\ &+\boldsymbol{\mathcal{C}}_{\tilde{\mathbf{p}}\mathbf{i}_{\mathbf{p}}}^{\mathcal{H}})\boldsymbol{\mathcal{D}}_K^{\mathcal{H}} + \boldsymbol{\mathcal{C}}_{\mathbf{i}_s\mathbf{i}_s}(n_\tau) + \boldsymbol{\mathcal{C}}_{\mathbf{i}_{\mathbf{p}}\mathbf{i}_{\mathbf{p}}}) + \boldsymbol{\mathcal{C}}_{\tilde{\mathbf{v}}_K\tilde{\mathbf{v}}_K}(n_\tau) \quad (5)\end{aligned}$$

where $\boldsymbol{\mathcal{C}}_{\mathbf{ab}}(n, n_\tau) = \mathcal{E}\{\mathbf{a}(n+n_\tau)\mathbf{b}^{\mathcal{H}}(n)\}$[1] for column vectors $\mathbf{a}$ and $\mathbf{b}$. Based on the comments 1) and 2) in Section II, for the lag $n_\tau \neq 0$, it is easy to obtain: $\boldsymbol{\mathcal{C}}_{\mathbf{s}_M\mathbf{s}_M}(n_\tau) = 0$, $\boldsymbol{\mathcal{C}}_{\mathbf{s}_M\mathbf{i}_s}(n_\tau) = 0$, $\boldsymbol{\mathcal{C}}_{\mathbf{i}_s\mathbf{i}_s}(n_\tau) = 0$, $\boldsymbol{\mathcal{C}}_{\tilde{\mathbf{v}}_K\tilde{\mathbf{v}}_K}(n_\tau) = 0$, then (5) can be represented as

$$\boldsymbol{\mathcal{C}}_{\tilde{\mathbf{y}}_K\tilde{\mathbf{y}}_K}(n, n_\tau \neq 0) = \Phi^{n_\tau J}\mathbf{\Psi}_0 \quad (6)$$

where

$$\mathbf{\Psi}_0 = \boldsymbol{\mathcal{D}}_K\boldsymbol{\mathcal{C}}_{\tilde{\mathbf{p}}\tilde{\mathbf{p}}}\boldsymbol{\mathcal{D}}_K^{\mathcal{H}} + \boldsymbol{\mathcal{D}}_K\boldsymbol{\mathcal{C}}_{\tilde{\mathbf{p}}\mathbf{i}_{\mathbf{p}}} + \boldsymbol{\mathcal{C}}_{\tilde{\mathbf{p}}\mathbf{i}_{\mathbf{p}}}^{\mathcal{H}}\boldsymbol{\mathcal{D}}_K^{\mathcal{H}} + \boldsymbol{\mathcal{C}}_{\mathbf{i}_{\mathbf{p}}\mathbf{i}_{\mathbf{p}}} \quad (7)$$

We can see that the matrix $\mathbf{\Psi}_0$ is constant with respect to the lag n_τ. Therefore, $\boldsymbol{\mathcal{C}}_{\tilde{\mathbf{y}}_K\tilde{\mathbf{y}}_K}(n, n_\tau > 0)$ is a periodic function of n_τ with the period of $\frac{K}{J\phi}$ by assuming that the matrix $\mathbf{\Psi}_0$ is not zero (justification of this assumption will be given later). For $n_\tau \in (0, N-1]$, we perform the DFT on (6) and obtain (see [11] for DFT property)

$$\begin{aligned}&\tilde{\boldsymbol{\mathcal{C}}}_{\tilde{\mathbf{y}}_K\tilde{\mathbf{y}}_K}(n, m_\tau) \\ =\ &\frac{1}{N-1}\sum_{n_\tau=1}^{N-1}\boldsymbol{\mathcal{C}}_{\tilde{\mathbf{y}}_K\tilde{\mathbf{y}}_K}(n, n_\tau)e^{-j\frac{2\pi}{N-1}m_\tau n_\tau} \\ =\ &e^{-j\frac{2\pi}{N-1}(m_\tau - \frac{(N-1)J\phi}{K})}\mathbf{\Psi}_0\mathcal{S}(m_\tau - \frac{(N-1)J\phi}{K}) \quad (8)\end{aligned}$$

where

$$\mathcal{S}(x) = \frac{\sin(\pi x)}{(N-1)\sin(\frac{\pi}{N-1}x)}e^{-j\frac{N-2}{N-1}\pi x}$$

For $m_\tau \geqslant 0$, the norm of $\tilde{\boldsymbol{\mathcal{C}}}_{\tilde{\mathbf{y}}_K\tilde{\mathbf{y}}_K}(n, m_\tau)$ is given by

$$\|\tilde{\boldsymbol{\mathcal{C}}}_{\tilde{\mathbf{y}}_K\tilde{\mathbf{y}}_K}(n, m_\tau)\| = \|\mathbf{\Psi}_0\||\mathcal{S}(m_\tau - \frac{(N-1)J\phi}{K})| \quad (9)$$

[1] If $\mathbf{a}(n)$ and $\mathbf{b}(n)$ are wide-sense stationary, then $\boldsymbol{\mathcal{C}}_{\mathbf{ab}}(n, n_\tau)$ is not the function of n and expressible as $\boldsymbol{\mathcal{C}}_{\mathbf{ab}}(n_\tau)$. If $\mathbf{a}(n)$ and $\mathbf{b}(n)$ are constant, then we can express $\boldsymbol{\mathcal{C}}_{\mathbf{ab}}(n, n_\tau) = \boldsymbol{\mathcal{C}}_{\mathbf{ab}}$.

which achieves its maximum along the m_τ direction only when $|\mathcal{S}(m_\tau - \frac{(N-1)J\phi}{K})|$ reaches its maximum, ie. $m_\tau - \frac{(N-1)J\phi}{K} = 0$. Since m_τ is an integer, the maximum of $|\mathcal{S}(m_\tau - \frac{(N-1)J\phi}{K})|$ should located at

$$\hat{m}_\tau = \lfloor \frac{(N-1)J\phi}{K} + \frac{1}{2} \rfloor \tag{10}$$

where $\lfloor \cdot \rfloor$ denotes the integer floor. Hence, we can first determine such a $\hat{m}_\tau$ by searching the maximum of $\|\tilde{\boldsymbol{\mathcal{C}}}_{\tilde{\mathbf{y}}_K\tilde{\mathbf{y}}_K}(n, m_\tau)\|$ over $m_\tau \in [0, N-2]$. Then, the NCFO can be estimated via

$$\hat{\phi} = \frac{K\hat{m}_\tau}{(N-1)J} \tag{11}$$

Then, we provide three comments:

3.1.1. Estimation range

For $m_\tau \in [0, N-2]$, the maximum identifiable NCFO, denoted by $\hat{\phi}_{\max}$, can be derived from (11)

$$\hat{\phi}_{\max} = \frac{(N-2)K}{(N-1)J} \tag{12}$$

Due to the effect of frequency fold, the estimate range of CFO is given by $|\phi| \leqslant \lfloor \frac{(N-2)K}{2(N-1)J} \rfloor$.

3.1.2. Quantization noise

Since m_τ is an integer, the relationship between ϕ and m_τ can be derived from (10) and (11) as

$$\phi = \frac{K(m_\tau + \delta_M)}{(N-1)J} \tag{13}$$

where $|\delta_M| \leqslant 0.5$ is the quantization noise. This noise may incur the CFO estimation error as

$$|\hat{\phi} - \phi| = \frac{K|\delta_M|}{(N-1)J} \leqslant \frac{K}{2(N-1)J} \tag{14}$$

Certainly, this error can be further mitigated by increasing N.

3.1.3. Computation complexity

The computation complexity of the CS-based approach is mainly from the DFT operation. Even though it is usually replaced by FFT, (8) still needs the complexity of $\mathcal{O}(K^2(N-1)\log(N-1))$.

3.2. The LR-based estimator

The linear regression estimator is based on the following equation

$$\mathbf{C}(n, n_\tau) = \boldsymbol{\mathcal{C}}_{\tilde{\mathbf{y}}_K\tilde{\mathbf{y}}_K}(n, n_\tau)\boldsymbol{\mathcal{C}}^{\mathcal{H}}_{\tilde{\mathbf{y}}_K\tilde{\mathbf{y}}_K}(n, 1) = \Phi^{(n_\tau-1)J}\boldsymbol{\Gamma} \tag{15}$$

where $\boldsymbol{\Gamma} = \boldsymbol{\Psi}_0\boldsymbol{\Psi}_0^{\mathcal{H}}$ is a Hermitian matrix. The trace of $\mathbf{C}(n, n_\tau)$ is given by

$$\mathrm{Tr}\{\mathbf{C}(n, n_\tau)\} = \Phi^{(n_\tau-1)J}\mathrm{Tr}\{\boldsymbol{\Gamma}\} \tag{16}$$

Due to $\boldsymbol{\Psi}_0 \neq \mathbf{0}$, $\mathrm{Tr}\{\boldsymbol{\Gamma}\}$ should be positive. So, we can obtain the phase of $\mathrm{Tr}\{\mathbf{C}(n, n_\tau)\}$ using

$$\begin{aligned} \varphi(n_\tau) &= \arg\{\mathrm{Tr}\{\mathbf{C}(n, n_\tau)\}\} \\ &= \frac{2\pi J\phi}{K}(n_\tau - 1) - 2\pi\lfloor\frac{2n_\tau + T_\varphi}{2T_\varphi}\rfloor \end{aligned} \tag{17}$$

where $\arg\{x\}$ is a function to obtain the phase of x, for $\arg\{x\} \in [-\pi, \pi)$; $T_\varphi = \frac{K}{J\phi}$ is the period of the function $\varphi(n_\tau)$; Assuming T_φ to be known, we can form a first-order polynomial $f(n_\tau) = an_\tau + b$ and determine the parameters (a, b) by solving the following equation

$$(\hat{a}, \hat{b}) = \arg\min_{(\hat{a},\hat{b})} \sum_{n_\tau=1}^{\lfloor T_\varphi/2 \rfloor} |\varphi(n_\tau) - f(n_\tau)|^2 \tag{18}$$

It is easy to find that $\hat{a}$ is the estimated slope of $\varphi(n_\tau)$, which is identifiable by using the LR algorithm. Then, the NCFO ϕ can be determined by

$$\hat{\phi} = \frac{K}{2\pi J}\hat{a} \tag{19}$$

The following points should be noted for the LR-based approach:

3.2.1. Estimation performance

Eqn. (18) shows that the curve fitting performance improves with the increase of T_φ. However, T_φ is inverse proportional to the NCFO. Hence, the estimation performance becomes worse with the increase of NCFO.

3.2.2. About $\lfloor T_\varphi/2 \rfloor$

(18) shows that the knowledge of $\lfloor T_\varphi/2 \rfloor$ is required for the successful CFO estimation. To determine $\lfloor T_\varphi/2 \rfloor$, we perform the differential operation on $\varphi(n_\tau)$ and have

$$\begin{aligned} \Delta\varphi(n_\tau) &= \varphi(n_\tau + 1) - \varphi(n_\tau) \\ &= \begin{cases} \gamma, & \text{for } n_\tau = \lfloor (2i+1)T_\varphi/2 \rfloor \\ \frac{2\pi J\phi}{K}, & \text{otherwise} \end{cases} \end{aligned} \tag{20}$$

where $i = 0, 1, \cdots$, and γ is very close or equal to -2π [2]. Due to $|\frac{2\pi J\phi}{K}| << |\gamma|$, we can find $\lfloor T_\varphi/2 \rfloor$ by searching the first location of γ over $n_\tau \in (0, N-1)$. If there does not have such a γ, then we set $\lfloor T_\varphi/2 \rfloor = N-1$.

[2] $\gamma = -2\pi$ holds only when T_φ is an integer.

3.3. About $\mathbf{\Psi}_0$

In order to guarantee the CFO identifiability, we need the condition: $\mathbf{\Psi}_0 \neq \mathbf{0}$. Because $\tilde{\mathbf{p}}$ and $\mathbf{i_p}$ are constant, (7) can be rewritten into

$$\mathbf{\Psi}_0 = \boldsymbol{\mathcal{D}}_K \tilde{\mathbf{p}} \tilde{\mathbf{p}}^{\mathcal{H}} \boldsymbol{\mathcal{D}}_K^{\mathcal{H}} + \boldsymbol{\mathcal{D}}_K \tilde{\mathbf{p}} \mathbf{i}_{\mathbf{p}}^{\mathcal{H}} + \mathbf{i_p} \tilde{\mathbf{p}}^{\mathcal{H}} \boldsymbol{\mathcal{D}}_K^{\mathcal{H}} + \mathbf{i_p} \mathbf{i}_{\mathbf{p}}^{\mathcal{H}} \quad (21)$$

In order to assure $\mathbf{\Psi}_0 \neq \mathbf{0}$, the pilot design should fulfill $\boldsymbol{\mathcal{D}}_K \tilde{\mathbf{p}} = \mathbf{0}$. Since $\boldsymbol{\mathcal{D}}_K$ contains at most L_u zeros on its diagonal, this condition can be achieved when $\tilde{\mathbf{p}}$ has at least $L_u + 1$ nonzero elements.

4. SIMULATION RESULTS AND ANALYSIS

The root mean-square error (RMSE), $\sqrt{1/\mathcal{I} \sum_{i=0}^{\mathcal{I}-1} |\hat{\phi}_i - \phi|^2}$, were used to benchmark the CFO estimation performance. Here, $\mathcal{I}$ is the number of Monte Carlo trials. The frequency-selective fading channel was modelled as a FIR filter with the maximum order of $L_u = 4$. Each tap was randomly generated according to the Rayleigh distribution with the variance of $1/(L_u + 1)$. The block precoder $\mathbf{W}$ was formed by the $K \times K$ Walsh matrix. The parameters of GMC-CDMA systems were given by: $K = 32$, $M = 28$, $L_{\rm cp} = 4$, $L_t = 4$. The information-bearing symbols were drawn from the QPSK constellation with the equal probability. The sub-carrier spacing, Δf, of 312.5KHz, was the same as HIPERLAN/2 [14]. Elements in the pilot block $\mathbf{p}$ were identical. The pilot-to-information power ratio was given by L_t/M. The signal-to-noise ratio (SNR) is defined by the average received symbol energy to noise $E_s/\mathcal{N}_o$ [15]. Based on the above parameters, we find that the block $\tilde{\mathbf{p}}$ results in eight non-zero elements with the equal amplitudes. As shown in Sec. III-C, the CFO identifiability can be guaranteed by employing this kind of pilot design.

`Test Case 1:` This experiment examines the estimation performance as a function of NCFO with SNR=5 and 15dB respectively. The RMSE results were obtained by taking average of $\mathcal{I} = 500$ Monte Carlo trials. Each trial collected $N = 200$ GMC-CDMA blocks for the CFO estimation. Fig. 2 shows that the RMSE for the CS-based approach is very stable (around 2×10^{-3}). This result has a good match with the quantization error in (14). In the range of large NCFO (e.g. $|\phi| > 0.15$), we can observe that the LR-based approach cannot offer a good estimation due to the relatively short T_φ. The estimation performance improves significantly with the decrease of NCFO. When NCFO is small (e.g. $|\phi| < 0.1$), the LR-based approach outperforms the CS-based approach.

`Test Case 2:` To evaluate the sub-estimators for different SNR cases, we plot the RMSE results in Fig. 3 with the NCFO $\phi = 0.0625$ and the data record length $N = 100$ blocks. Fig. 3 shows that the CS-based sub-estimator is not sensitive to the SNR. The RMSE result for the LR-based estimator becomes stable and offers the best performance for SNR$>$ 10dB. In order to compare with stat-of-the-art approaches, we also plot the RMSE results for the pulse-shaping [9] based CFO estimators. Fig. 3 shows that the proposed estimators outperform the pulse-shaping based.

`Test Case 3:` In order to indicate the performance-complexity tradeoff, we examine the RMSE results as a function of data record length N with $\phi = 0.0625$ and the typical SNR$=$ 12dB. Fig. 4 shows that RMSE for CFO estimators decreases rapidly with the increase of N. They can achieve the best performance offered by the pulse-shaping based approach only using $N = 20$ blocks.

5. CONCLUSIONS

Utilizing the hidden pilots, this paper has proposed a novel CFO estimators for GMC-CDMA in unknown frequency-selective channels. It has been established that the CFO is identifiable in the frequency-domain by employing the CS and LR-based approaches. Both theoretical and simulation results have shown the excellent estimation performance of the proposed CFO estimator.

6. REFERENCES

[1] Z. Wang, and G. B. Giannakis, "Wireless multicarrier communications: Where Fourier meets Shannon," *IEEE Signal Processing Magzine*, May 2000.

[2] G. B. Giannakis, Z. Wang, A. Scaglione, and S. Barbarossa, "AMOUR-Generalized multicarrier transceiver for blind CDMA regardless of multipath," *IEEE Trans. on Communications*, vol. 48, pp. 2064-2076, Dec. 2000.

[3] T. Pollet, M. V. Bladel, and M. Moeneclaey, "BER sensitivity of OFDM systems to carrier frequency offset and Wiener phase noise," *IEEE Trans. on Communications*, vol. 43, pp. 191-193, Feb. 1995.

[4] F. Mazzenga, "Channel estimation and equalization for M-QAM transmission with a hidden pilot sequence," *IEEE Trans. on Broadcasting*, vol. 46, pp. 170-176, June 2000.

[5] J. K. Tugnait, and W. Luo, "On channel estimation using superimposed training and first-order statistics," *IEEE Communication Letters*, vol. 7, pp. 413-415, Sep. 2003.

[6] J. Li, G. Liu and G. B. Giannakis, "Carrier frequency offset estimation for OFDM-based WLAN," *IEEE Signal Processing Letters*, vol. 8, pp. 80-82, March 2001.

[7] J.-J. van. de Beck, etc.al, "A time and frequency synchronization scheme for multiuser OFDM," *IEEE JSAC*, vol. 17, No. 11, Nov. 1999.

[8] ——, "ML estimation of timing and frequency offset in OFDM systems," *IEEE Trans. on Signal Processing*, vol. 45, pp. 1800-1805, July 1997.

[9] H. Bolcskei, "Blind estimation of symbol timing and carrier frequency offset in wireless OFDM systems," *IEEE Trans. on Communications*, vol. 49, pp. 988-999, June 2001.

[10] N. Lashkarian and S. Kiaei, "Class of cyclic-based estimators for frequency offset estimation of OFDM systems," *IEEE Trans. on Communications*, vol. 48, pp. 2139-2149, Dec 2000.

[11] A. V. Oppenheim and R. W. Schafer, "Discrete-time signal processing," Prentice-Hall, Englewood Cliffs, New Jersey, USA, 1989.

[12] F. Gini and G. B. Giannakis, "Frequency offset and symbol timing recovery in flat-fading channels: A cyclostationary approach," *IEEE Trans. on Communications*, vol. 46, pp. 400-411, Mar. 1998.

[13] Y. Zhao, and S. G. Haggman "Intercarrier interference self-cancellation scheme for OFDM mobile communication systems," *IEEE Trans. on Communications*, vol. 49, pp. 1185-1191, July 2001.

[14] ETSI, "Broadband radio access networks (BRAN); high performance radio local area networks (HIPERLAN) Type 2: physical layer," document DTS0023003, France Dec 1999.

[15] J. Proakis, *Digital Communications*, 4th ed., New York: McGraw-Hill, 2000.

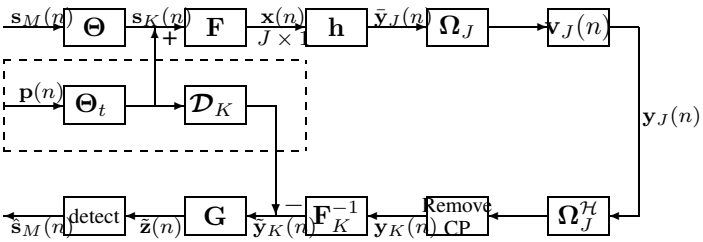

Fig. 1. Discrete-time equivalent model of GMC-CDMA with CFO and hidden pilots.

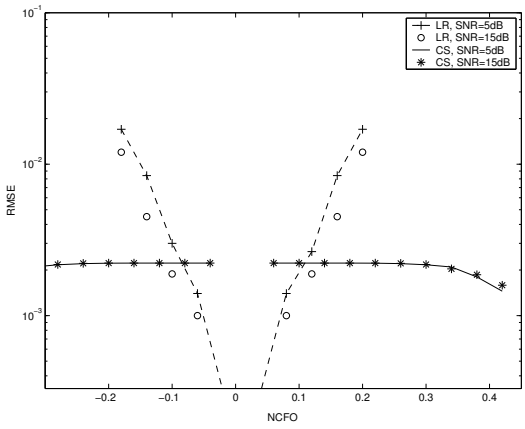

Fig. 2. RMSE results as a function of NCFO.

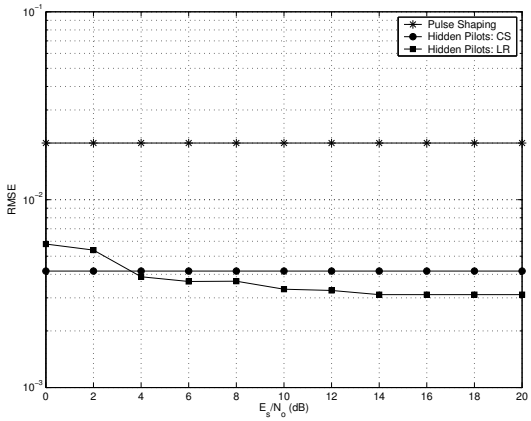

Fig. 3. RMSE results as a function of SNR ($\phi = 0.0625, N = 100$).

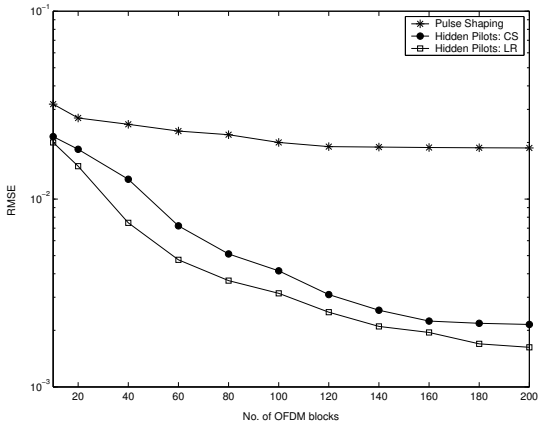

Fig. 4. RMSE results as a function of data record length ($\phi = 0.0625$, SNR=12dB).